

## Origin of Bellerophon states in globally coupled phase oscillators

Can Xu,<sup>1</sup> Stefano Boccaletti,<sup>2</sup> Shuguang Guan,<sup>3,\*</sup> and Zhigang Zheng<sup>1,†</sup>

<sup>1</sup>*Institute of Systems Science and College of Information Science and Engineering, Huaqiao University, Xiamen 361021, China*

<sup>2</sup>*CNR-Institute of Complex Systems, Via Madonna del Piano, 10, 50019 Sesto Fiorentino, Florence, Italy*

<sup>3</sup>*Department of Physics, East China Normal University, Shanghai 200241, China*



(Received 28 August 2018; published 26 November 2018)

We unveil the basic mechanisms and general conditions for the emergence of Bellerophon states, which are higher order coherent states appearing in globally coupled phase oscillators. The critical points for the involved phase transitions are determined analytically. The significant feature of Bellerophon states is that the oscillators' effective frequencies are locked to quantized plateaus, a point which is fully clarified on the basis of circle map theory. Each quantized plateau corresponds to a harmonic frequency of the Fourier decomposition of the order parameter. Our approach exploits the fact that the order parameter is always real, due to a special symmetry of the system which furthermore prevents the formation of even integer multiple plateaus of effective frequencies.

DOI: [10.1103/PhysRevE.98.050202](https://doi.org/10.1103/PhysRevE.98.050202)

Synchronization is one of the most common self-organization phenomena that can be observed in nature. To quote only a few examples of physical, biological, and social systems where synchrony spontaneously emerges from the interaction of unitary elements, one can refer to Josephson junction arrays [1,2], power grids [3], neurons in the brain [4–6], circadian rhythms of plants and animals [7], fireflies flashing [8], etc.

A prototypic model for the description of synchrony was introduced by Kuramoto [9], and for over four decades this model and some generalizations of it have been extensively studied [10–12]. Despite the simplicity of Kuramoto-like models, very rich scenarios of coherent states can be identified, which may include synchronized states [9], clustered states [13,14], traveling-wave states,  $\pi$  and standing-wave states [15,16], glass and spurious glass states [17,18], splay states [19,20], and higher order forms of entrainment [21,22].

Recently, the attention focused on two nontrivial states, namely, the chimera and the Bellerophon (B) state. The original chimera state referred to the coexistence of domains of coherent and incoherent dynamics in *locally coupled identical* oscillators [23,24], while later more complicated structures were identified such as the breathing chimera state [25], the clustered chimera state [26], and the multichimera state [27]. When, instead, *globally coupled nonidentical* oscillators are considered and the coupling strength in Kuramoto models is correlated with the natural frequency, a time-dependent and clustered state (the Bellerophon state) is observed [28]. The most important feature of such a latter state is that the system forms quantized clusters. Inside each cluster the instantaneous speeds of the oscillators are not locked. However, the average speeds of the oscillators converge to a common value for a long-time evolution. Further studies revealed that the emergence of this state is robust to natural frequency distributions and coupling schemes [29–31]. When compared with typical

stationary coherent states, such as the (partially) synchronized states and the traveling-wave states, B states represent actually a higher order form of coherence. It should be pointed out that B states are essentially different from the other higher coherence previously reported [21,22]. First, B states are self-organized in coupled autonomous oscillators, while the clustering coherence observed in Refs. [21,22] occurs in systems with external forces. Second, in B states coherent oscillators always appear in pairs, while in the latter states they do not.

In this Rapid Communication, we provide the general conditions for the formation of Bellerophon states, and elucidate their dynamical behaviors both analytically and numerically. To this end, we refer to a Kuramoto model of globally coupled oscillators with in and out frequency-weighted coupling. Namely, we focus on the transitions associated with several states induced by this particular coupling, and show that B states correspond in fact to periodic solutions of the system. We reveal that the critical mean-field frequency and the coupling pattern are the key parameters determining the emergence of such oscillatory states, which occur in the regime of intermediate coupling strength where the incoherent state is unstable and the zero-frequency clustered state is empty. Furthermore, the quantized nature of plateaus in the average frequencies can be fully explained in terms of the circle map theory, where such a simple structure is caused by the property of Riccati's equation. Finally, we prove that the traveling-wave state (i.e., the nonzero-frequency partial synchronized state) can never take place in the model.

Let us then start with considering a generalized Kuramoto model, describing the dynamics of an ensemble of  $N$  globally coupled phase oscillators:

$$\dot{\theta}_i = \omega_i + \frac{K_i}{N} \sum_{j=1}^N G_j \sin(\theta_j - \theta_i), \quad i = 1, \dots, N, \quad (1)$$

where the dot stands for the temporal derivative, and  $\theta_i$  and  $\omega_i$  are, respectively, the instantaneous phase and the natural frequency of the  $i$ th oscillator. The set of frequencies  $\{\omega_i\}$  are extracted from a probability density function  $g(\omega)$  in the

\*sgguan@phy.ecnu.edu.cn

†zgzhenq@hqu.edu.cn

limit  $N \rightarrow \infty$ .  $K_i$  and  $G_j$  are in- and out-coupling strength which both cause heterogeneity in the system [32]. We here consider a class of coupling patterns, the frequency-weighted one, where the in- and out-coupling strengths are proportional to the absolute value of the nodes' natural frequencies. Two distinct cases will be discussed: the in-coupling weighted (where  $K_i = \kappa|\omega_i|$  and  $G_j \equiv 1 \forall j$ ) and the out-coupling weighted (where  $K_i \equiv 1 \forall i$  and  $G_j = \kappa|\omega_j|$ ) configurations, both having  $\kappa > 0$ .

For simplicity, let us start with the in-coupling weighted case. The level of synchronization can be monitored by the order parameter  $z(t) = R(t)e^{i\Psi(t)} = \frac{1}{N} \sum_{j=1}^N e^{i\theta_j(t)}$ .  $z(t)$  is the average of the complex amplitudes  $e^{i\theta_j(t)}$ ,  $R(t)$  is the module of  $z(t)$  (reflecting coherence of the oscillators' instantaneous phases), and  $\Psi(t)$  is the averaged phase. One can assume that the mean-field phase  $\Psi$  rotates uniformly with frequency  $\Omega$ , i.e.,  $\Psi(t) = \Omega t + \Psi(0)$ . In this rotating frame with frequency  $\Omega$ , following the treatment in Ref. [33] [Eqs. (3)–(20) in [33]], one can obtain the self-consistent equations for the mean field  $(R, \Omega)$  as

$$R = \int_{-\infty}^{\infty} d\omega g(\omega) \sqrt{1 - \left(\frac{\omega - \Omega}{\kappa R \omega}\right)^2} \Theta\left(1 - \left|\frac{\omega - \Omega}{\kappa R \omega}\right|\right) \quad (2)$$

and

$$0 = \int_{-\infty}^{\infty} d\omega g(\omega) \frac{\omega - \Omega}{\kappa R |\omega|} - \int_{-\infty}^{\infty} d\omega g(\omega) \times \sqrt{\left(\frac{\omega - \Omega}{\kappa R \omega}\right)^2} - 1 \Theta\left(\left|\frac{\omega - \Omega}{\kappa R \omega}\right| - 1\right), \quad (3)$$

where  $\Theta(x)$  is the Heaviside step function. Then the critical point, where the incoherent state loses its stability, can be obtained as  $\kappa_{c,1} = \frac{2}{\pi|\Omega_c|g(\Omega_c)}$ . Here  $\Omega_c$  is the critical mean-field frequency [33,34].

For the sake of illustration, let us take a bimodal Lorentzian distribution:

$$g(\omega) = \frac{\Delta}{2\pi} \left[ \frac{1}{(\omega - \omega_0)^2 + \Delta^2} + \frac{1}{(\omega + \omega_0)^2 + \Delta^2} \right]. \quad (4)$$

In this case, a pair of  $\Omega_c$  are obtained, namely,  $\Omega_c = \pm\sqrt{\omega_0^2 + \Delta^2}$ . Substituting  $\Omega_c$  into the equation for  $\kappa_{c,1}$  yields

$$\kappa_{c,1} = 4 \sqrt{1 + \left(\frac{\omega_0}{\Delta}\right)^2}. \quad (5)$$

From the solution, it appears that  $\kappa_{c,1}$  is inversely proportional to the dimensionless parameter  $\omega_0/\Delta$ , and the physical picture can be understood as follows. When  $\omega_0 = 0$ , the distribution is actually unimodal, and the natural frequencies of most oscillators are centered around zero. Consequently, a maximum of  $\kappa_{c,1} = 4$  is expected, in order to make the effective coupling strength  $\kappa R|\omega_i|$  exceed the threshold for entraining oscillators in the system. As  $\omega_0/\Delta$  exceeds  $\sqrt{3}/3$ ,  $g(\omega)$  becomes bimodal and thus the natural frequencies of most oscillators clusterize around  $\pm\omega_0$ . This latter fact contributes a larger factor in the effective coupling strength, and therefore a smaller  $\kappa_{c,1}$  is enough to induce phase coherence.

On the other hand, one finds that  $\Omega \equiv 0$  is always a trivial solution of Eq. (3). Combining with Eq. (2), a cluster partially synchronized state can be solved, which occurs at  $\kappa_{c,2} = 2$

with [35]

$$R_{\pm} = \frac{\sqrt{2}}{2} \sqrt{1 \pm \sqrt{1 - \frac{4}{\kappa^2}}}, \quad \kappa \geq \kappa_{c,2}. \quad (6)$$

To get insights on the dynamical stability of  $R_{\pm}$ , one can analyze the system based on the Ott-Antonsen (OA) ansatz [36–38]. In the thermodynamical limit  $N \rightarrow \infty$ , a probability density function  $\rho(\theta, \omega, t)$  can be defined that represents the fraction of oscillators with frequency  $\omega$  having, at time  $t$ , an instantaneous phase between  $\theta$  and  $\theta + d\theta$ . Considering the  $2\pi$  periodicity with respect to  $\theta$ ,  $\rho(\theta, \omega, t)$  can be expanded as a Fourier series  $\rho(\theta, \omega, t) = \frac{g(\omega)}{2\pi} (1 + \rho_+ + \rho_-)$ , where  $\rho_+ = \sum_{n=1}^{\infty} \tilde{\alpha}^n(\omega, t) e^{in\theta}$ , and  $\rho_- = \tilde{\rho}_+$ .  $\alpha(\omega, t)$  is the first Fourier coefficient of  $\rho(\theta, \omega, t)$ , denoting the suborder parameter at a given frequency  $\omega$ . Accordingly, the global order parameter becomes  $z(t) = \int_{-\infty}^{\infty} g(\omega) \alpha(\omega, t) d\omega$ . Following the OA ansatz [36,37], the evolution of  $\alpha(\omega, t)$  is ruled by

$$\frac{\partial \alpha(\omega, t)}{\partial t} = i\omega \alpha(\omega, t) + \frac{\kappa|\omega|}{2} [z(t) - \alpha^2(\omega, t)] \bar{z}(t), \quad (7)$$

where  $\bar{z}$  denotes the complex conjugation of  $z$ .

An analytical continuation for the frequency-weighted Kuramoto model is hampered by the fact that  $|\omega|$  in Eq. (7) is not an analytic function. Therefore, the system cannot be further reduced into a low-dimensional dynamics described by a few ordinary differential equations. However, one can still analyze the stability of solutions of Eq. (6) based on Eq. (7). Defining  $\alpha_p(t)$  [ $\alpha_n(t)$ ] as the suborder parameter contributed by all oscillators with natural frequency  $\omega > 0$  ( $\omega < 0$ ), one can obtain the following governing equations:

$$\dot{\alpha}_{p,n} = i\omega \alpha_{p,n} + \frac{\kappa|\omega|}{2} R (1 - \alpha_{p,n}^2), \quad (8)$$

which admit, as stationary solutions,

$$\alpha_{p,n}^* = \sqrt{1 - \left(\frac{1}{\kappa R}\right)^2} \pm i \frac{1}{\kappa R}. \quad (9)$$

As  $\alpha_{p,n} \rightarrow \alpha_{p,n}^*$ ,  $R \rightarrow R_{\pm}$ . From Eq. (6), it is easy to verify that  $\kappa R > 1$ . Physically,  $\alpha_{p,n}^*$  just corresponds to the complex amplitude of two phase-locked clusters on the unit circle [see Fig. 2(b) in Ref. [35]]. Letting  $y = \alpha_p(t)/\alpha_n(t)$ , one has

$$\dot{y} = 2i|\omega|y + \frac{\kappa|\omega|}{2} (1 - y^2). \quad (10)$$

The eigenvalue for the stationary state is  $\lambda = -\kappa|\omega|(1 - \frac{2}{1-R^2})$ . Further analysis indicates that  $\lambda(R_+) < 0$  and  $\lambda(R_-) > 0$ , which implies that the solution  $R_+$  is stable. Therefore, the OA manifold contains a particular direction where partially synchronous state  $R_-$  is unstable with the separation of two cluster phase-locked oscillators.

Notice that there is no guarantee that  $\Omega \equiv 0$  is the only solution Eq. (3) [39,40], as at least  $\Omega_c = \pm\sqrt{\omega_0^2 + \Delta^2} \neq 0$  are also solutions. However, a traveling-wave solution  $\Omega \neq 0$  is not found in the system. Although a general analysis on the existence and stability of traveling-wave solutions in the frequency-weighted Kuramoto model is very problematic [41], the local bifurcation information of the traveling-wave solution near the critical point  $\kappa_{c,1}$  can still be captured. On the one hand, including the high-order terms of Taylor series

in Eq. (2) ( $\Omega \rightarrow \Omega_c, \kappa \rightarrow \kappa_c$ ), the critical behavior of  $R$  with  $\Omega \approx \Omega_c$  (traveling-wave solution) is

$$R = \sqrt{-\frac{8}{\pi\beta} \frac{\delta\kappa}{\kappa_c^4}}, \quad (11)$$

where  $\beta = 3\Omega_c g(\Omega_c) + 3\Omega_c^2 g'(\Omega_c) + \frac{1}{2}\Omega_c^3 g''(\Omega_c)$  (the bifurcation is subcritical when  $\beta > 0$ , and supercritical for  $\beta < 0$ ). On the other hand, further information on local bifurcation and stability can be gathered by the use of the Crawford central manifold theory [42]. It is found that for the frequency-weighted model, the system undergoes a Hopf bifurcation near the critical coupling  $\kappa_{c,1}$ . As a result, a traveling-wave solution and a standing-wave solution emerge above  $\kappa_{c,1}$  [33]. Provided  $g(\omega)$  is even, the traveling-wave solution is always locally unstable. One can then conclude that the system tends to a stationary solution with  $\Omega \equiv 0$ . Furthermore, when  $|\Omega_c|g(\Omega_c) < 1/\pi$ , the system undergoes a first-order phase transition such as in the cases of the unimodal Lorentzian, triangle, and Gaussian distributions [34].

When  $|\Omega_c|g(\Omega_c) > 1/\pi$ , an oscillatory state emerges in the middle regime of coupling strength ( $\kappa_{c,1} < \kappa < \kappa_{c,2}$ ), for both the uniform and the bimodal Lorentzian distribution ( $\omega_0 > \Delta/\sqrt{3}$ ). Such a state was termed as the B state in Ref. [28]. It is a quantized, time-dependent, clustered and coherent phase. The most important characteristic of B states is that inside each cluster, the oscillators' instantaneous frequencies are not locked, but their long-time averages (i.e., the effective frequencies) converge into a fixed value. Furthermore, symmetric quantized plateaus of effective frequencies emerge, made of an integer multiple of a principal frequency.

In previous studies of ours [28,30], these features of B states were characterized in detail. However, the mechanism underlying such a higher order coherence was still elusive. Motivated by the work in Ref. [43], in the following we move to reveal the reasons why B states display such dynamical traits and features.

Without loss of generality, we take the in-coupling case as an example. As the order parameter for B states is time dependent, the angular speed of each oscillator can be written as

$$\dot{\theta} = \omega + \kappa|\omega|\text{Im}[z(t)e^{-i\theta}]. \quad (12)$$

Note that the index  $i$  is replaced here by the frequency  $\omega$  since  $N \rightarrow \infty$ . In addition, we emphasize that it does not matter whether  $z(t)$  is a driving force from outside or some ensemble average quantity (such as an order parameter). What matters is instead that  $z(t)$  be the same for all  $\omega$  and be periodic in time [ $z(t+T) = z(t)$  for a given period  $T$ ]. According to Eq. (12), the effective frequency for each  $\omega$  is defined by  $\omega_{\text{eff}} = \lim_{t \rightarrow \infty} \theta(t)/t$ .

The flow map of Eq. (12) is defined as Poincaré map  $f_\omega$ , which charts (in each period) the initial phase  $\theta_0 = \theta(0)$  to another phase on the unit circle, i.e.,  $f_\omega(\theta_0) = \theta(T)$ . The circle map  $f_\omega : \mathbf{S}^1 \rightarrow \mathbf{S}^1$  is an orientation-preserving diffeomorphism, and it is helpful to lift the circle map to  $\mathbf{R}$  [44], i.e.,  $e^{iF_\omega(\theta)} = f_\omega(e^{i\theta})$ ,  $\theta \in \mathbf{R}$ . The circle map lift  $F_\omega : \mathbf{R} \rightarrow \mathbf{R}$  is strictly increasing, and satisfies  $F_\omega(\theta + 2\pi) = F_\omega(\theta) + 2\pi$ . Moreover,  $F_\omega(\theta) - \theta$  is a periodic function on  $\mathbf{R}$  with period  $2\pi$ .

The rotation number of  $F_\omega$  is defined as  $\text{rot}(F_\omega) = \lim_{n \rightarrow \infty} F_\omega^n(\theta)/n$ . According to the circle map theory, the rotation number  $\text{rot}(F_\omega)$  exists and does not depend on the initial phase  $\theta$ . It is easy to check that  $\omega_{\text{eff}} = \text{rot}(F_\omega)/T$  [43]. If a  $q$ -periodic solution for  $f_\omega$  exists, then  $f_\omega^q(\theta_0) = \theta_0$  for  $\theta_0 \in \mathbf{S}^1$ , which implies  $F_\omega^q(\theta_0) = \theta_0 + 2\pi p$ ,  $\theta_0 \in \mathbf{R}$  where  $p, q \in \mathbf{Z}$ . Then, the rotation number becomes  $\text{rot}(F_\omega) = 2\pi p/q$ .

Now, if the lift  $F_\omega^q(\theta)$  intersects with the straight line  $y = \theta + 2\pi p$  at a point  $(\theta_0, \theta_0 + 2\pi p)$  a nonempty interval of  $\omega$  must exist (according to the implicit function theorem) in which the curves always intersect, except for the case of  $F_\omega^q(\theta)$  being an identical map. This latter property warrants that for a generalized circle map lift  $F_\omega$  the rotation number always exhibits a ‘‘devil’s staircase’’ structure, where the plateaus appear for any rational fraction  $2\pi p/q$  [44].

The Kuramoto-like model considered here is, in fact, simple to treat. If we let  $y = e^{i\theta}$  (i.e.,  $\dot{y} = iy\dot{\theta}$ ), Eq. (12) becomes

$$\dot{y} = -\frac{1}{2}\kappa|\omega|\bar{z}y^2 + i\omega y + \frac{1}{2}\kappa|\omega|z, \quad (13)$$

which is a typical Riccati equation on the extended complex plane [45]. Furthermore, if one sets

$$y(t) = \frac{2}{\kappa|\omega|\bar{z}} \frac{\dot{x}(t)}{x(t)}, \quad (14)$$

then the Riccati equation is closely related to the following second-order linear differential equation:

$$\ddot{x} - \left(\frac{\dot{z}}{z} + i\omega\right)\dot{x} - \frac{1}{4}[\kappa|\omega|R(t)]^2 x = 0. \quad (15)$$

Accordingly, due to the linear superposition principle, a solution of the Riccati equation is the Möbius transformation of the inner parameters.

The Möbius transformation is the linear fractional map, which preserves the unit disk and can be classified into three types: elliptic (conjugate to a rotation of the disk), hyperbolic (having an attracting-repelling pair of fixed points on the circle), and parabolic (featuring a unique, globally attracting, fixed point on the circle) [43,46]. Therefore, all periodic solutions of  $f_\omega$  corresponding to  $|q| > 1$  are ruled out, and the quantized plateaus for the effective frequencies which are locked to  $2\pi k/T$  can only take place in the interval  $[\omega_k, \omega_{k+1}]$  [43].

Further observations indicate that the integer multiple  $k$  is odd in the frequency-weighted Kuramoto model. The latter can be explained as follows [43]. Due to the symmetry of  $g(\omega)$ , the system has a class of solution  $\theta_{-j}(t) = -\theta_j(t)$ . Then, the mean-field equation (12) becomes

$$\dot{\theta} = \omega - \kappa|\omega|R(t)\sin\theta. \quad (16)$$

Additionally, Eq. (16) is invariant under a translation  $\pi$  [where  $R(t)$  becomes  $-R(t)$ ]. Since  $R(t+T) = R(t)$ , then  $R(t)$  and  $-R(t)$  must be shifted by  $\frac{T}{2}$ , i.e.,  $R(t + \frac{T}{2}) = -R(t)$ . Therefore, if  $\theta(t)$  is a solution of Eq. (16), then  $\theta(t + \frac{T}{2}) + \pi$  is also a solution. In each plateau, the Möbius map is parabolic or hyperbolic, and has an attracting fixed point  $\theta(t)$  on the unit circle. Consequently, for the lift  $\theta(t + \frac{T}{2}) + \pi = \theta(t) + 2\pi n$ , the effective frequency is  $\frac{2\pi}{T}(2n - 1)$ ,  $n \in \mathbf{Z}$ .

In order to strengthen our arguments, we next study the case of out-coupling weights for Eq. (1), i.e.,  $G_j = \kappa |\omega_j|$  and  $K_i \equiv 1$ . There, one defines a weighted-order parameter

$$w(t) = D(t)e^{i\Phi(t)} = \frac{1}{N} \sum_{j=1}^N |\omega_j| e^{i\theta_j(t)}, \quad (17)$$

which constitutes another useful measure of phase coherence. Note that a one-body equation of  $\theta_i$  follows from Eq. (1) for each  $i$ ,

$$\dot{\theta}_i = \omega_i + \kappa D \sin(\Phi - \theta_i). \quad (18)$$

Next, one sets a self-consistent equation for  $D$ , and expresses  $R$  in terms of  $D$ . Following a method similar to the in-coupling case, and assuming that both  $R$  and  $D$  become asymptotically stationary ( $\dot{\Phi} = \Omega$ ), one can obtain the self-consistent equation for  $D$  and  $\Omega$  as

$$D = \int_{-\infty}^{\infty} d\omega |\omega| g(\omega) \sqrt{1 - \left( \frac{\omega - \Omega}{\kappa D} \right)^2} \Theta \left( 1 - \left| \frac{\omega - \Omega}{\kappa D} \right| \right) \quad (19)$$

and

$$0 = \int_{-\infty}^{\infty} d\omega |\omega| g(\omega) \frac{\omega - \Omega}{\kappa D} - \int_{-\infty}^{\infty} d\omega |\omega| g(\omega) \frac{\omega - \Omega}{\kappa D} \times \sqrt{1 - \left( \frac{\kappa D}{\omega - \Omega} \right)^2} \Theta \left( \left| \frac{\omega - \Omega}{\kappa D} \right| - 1 \right). \quad (20)$$

The order parameter  $R$  is

$$R = \int_{-\infty}^{\infty} d\omega g(\omega) \sqrt{1 - \left( \frac{\omega - \Omega}{\kappa D} \right)^2} \Theta \left( 1 - \left| \frac{\omega - \Omega}{\kappa D} \right| \right). \quad (21)$$

It should be pointed out that the first critical coupling  $\kappa_{c,1}$  for the emergence of a nonzero order parameter is the same as that for the in-coupling weighted case, whereas  $\Omega \equiv 0$  is always a trivial solution of Eq. (20) and it can be used to calculate the second critical coupling  $\kappa_{c,2}$ . For convenience, in the Lorentzian distribution we set  $\omega_0 = 0$  and  $\Delta = 1$  and obtain

$$D = \frac{2}{\pi} \left( \sqrt{1 + \left( \frac{1}{\kappa D} \right)^2} \operatorname{arcsinh}(\kappa D) - 1 \right). \quad (22)$$

The solutions of Eq. (22) individuate all stationary features of the out-coupling weighted case. From Fig. 1 it can be seen that the curves representing both sides of Eq. (22) have always a trivial intersection at  $(0, 0)$  for all  $\kappa$ . This implies that the incoherent state ( $D = R = 0$ ) is always a solution of the system. However, linear stability analysis suggests that the state  $D = R = 0$  is only stable in the regime  $0 < \kappa \leq \kappa_{c,1}$ . When  $\kappa > \kappa_{c,1}$ , the two curves have no other intersections, which means that the zero-frequency coherent state ( $D > 0$ ,  $0 < R \leq 1$ ,  $\Omega \equiv 0$ ) exists only when  $\kappa$  gets to  $\kappa_{c,2}$ . Remarkably,  $\kappa_{c,2}$  can be computed in the special case where the two curves plotting both sides of Eq. (22) are tangent (see Fig. 1). A pair of solutions exists in the regime  $\kappa > \kappa_{c,2}$ , expressed by  $D_+$  and  $D_-$ . With the increasing of  $\kappa$ ,  $D_+ \rightarrow \infty$  corresponds to

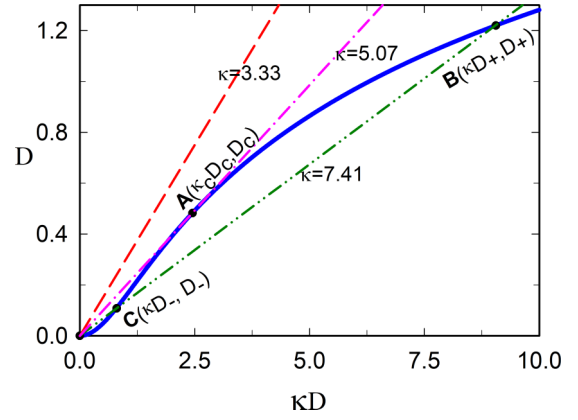


FIG. 1. Graphic method for the solution of Eq. (22). The blue curve represents the expression at the right-hand side of Eq. (22). The three lines correspond to the cases  $\kappa < \kappa_{c,2}$  (dashed red line),  $\kappa = \kappa_{c,2}$  (dash-dot pink line), and  $\kappa > \kappa_{c,2}$  (dash-dot-dot green line), respectively.

$R_+ = \frac{\sqrt{1 + (\kappa D_+)^2} - 1}{\kappa D_+} \rightarrow 1$ , which is the stable solution representing full synchronization. In addition,  $D_- \rightarrow 0$  leads to  $R_- \rightarrow 0$ , which is unstable, standing for desynchronization of the system [see Fig. 2(a)].

The emergence of B states follows a way similar to that of the in-coupling weighted case. On the one hand, the order parameters  $R(t)$  and  $D(t)$  are always real due to the symmetry  $[\theta_{-j}(t) = -\theta_j(t)]$ , and traveling-wave solutions ( $\Omega \neq 0$ ) are not permitted. On the other hand, since the incoherent state is unstable and the zero-frequency coherent state is empty when  $\kappa_{c,1} < \kappa < \kappa_{c,2}$ , the system undergoes a Hopf bifurcation near the critical point  $\kappa_{c,1}$ , and a B state is set [see Fig. 2(a)]. Actually, the B state is a special type of periodic solution of the system such that both order parameters  $R(t)$  and  $D(t)$  oscillate periodically. The real and periodic properties of  $R(t)$  and  $D(t)$  lead to special patterns of the effective frequencies [visible in Fig. 2(b)].

In conclusion, we studied large populations of globally coupled oscillators interacting with both in- and out-frequency weighted strengths. The emergence of oscillatory states is a

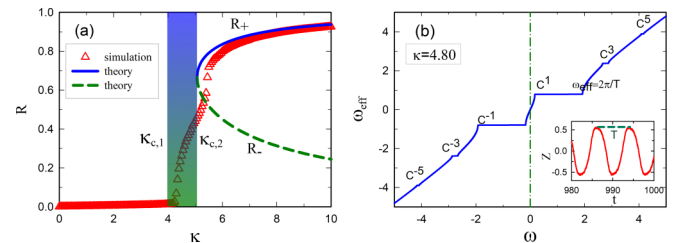


FIG. 2. (a) Phase diagram  $R$  vs  $\kappa$  for the out-coupling case with a Lorentzian distribution ( $\omega_0 = 0$  and  $\Delta = 1$ ). The dark-blue vertical region ( $\kappa_{c,1} < \kappa < \kappa_{c,2}$ ) is the area where B states emerge. The red triangles report the results of numerical simulation, while the curves labeled with  $R_+$  and  $R_-$  are the theoretic predictions. (b) A typical B state, observed at  $\kappa = 4.80$ . The panel reports the long-time average frequency  $\omega_{\text{eff}}$  of the oscillators vs their natural frequency  $\omega$ .  $C^k$  ( $k \in \mathbf{Z}$ ) are the different plateaus with index  $k$ . The inset reports the time evolution of the order parameter  $z(t)$ , and  $T$  is the value of the period. In both panels,  $N = 10000$ .

common phenomenon in such systems, and it occurs in the middle regime of coupling strength ( $\kappa_{c,1} < \kappa < \kappa_{c,2}$ ) where the incoherent state is unstable and the trivial partial synchrony state is empty. The two critical coupling strengths are obtained analytically in the frame of the Ott-Antonsen ansatz. The macroscopic and microscopic mechanisms behind these oscillatory states correspond to a class of periodic solutions of the system, and the quantized plateaus structure of effective frequencies is rooted in the characteristics of the Riccati equation. Moreover, it is shown that the symmetry of the system (which only preserves locked effective frequencies at odd integer multiples of a main rhythm) warrants a real value of the order parameter.

Let us emphasize the major contributions of our work which are different from what has already been unveiled in previous studies [20,28,30,31,33–35]. As a first difference, we highlight that so far the focus was mainly put on frequency-weighted Kuramoto models with out-coupling arrangements. In this Rapid Communication, instead, a comprehensive

analysis is given of both the in- and out-coupling configurations (the critical point  $\kappa_{c,1}$  is obtained for both the in- and out-coupling cases). In addition, a general criterion for the stability of the two-cluster state is established within the help of the Ott-Antonsen ansatz, while linear stability theory was typically used in previous works. In particular, we could prove that a traveling-wave state is forbidden in the model. Finally, we provided the general conditions for the formation of B states, and elucidated their quantized plateaus on the basis of circle map theory. Our analytical and numerical description will then be helpful to physicists for seeking such oscillatory states in a variety of other experimental and natural systems.

This work is partially supported by the National Natural Science Foundation of China (Grants No. 11875135, No. 11875132, and No. 11835003), the Scientific Research Funds of Huaqiao University (Grants No. 15BS401 and No. 600005-Z17Y0064), and the Natural Science Foundation of Shanghai (Grant No. 18ZR1411800).

- 
- [1] K. Wiesenfeld, P. Colet, and S. H. Strogatz, *Phys. Rev. Lett.* **76**, 404 (1996).
- [2] A. B. Cawthorne, P. Barbara, S. V. Shitov, C. J. Lobb, K. Wiesenfeld, and A. Zangwill, *Phys. Rev. B* **60**, 7575 (1999).
- [3] A. E. Motter, S. A. Myers, M. Anhel, and T. Nishikawa, *Nat. Phys.* **9**, 191 (2013).
- [4] F. Varela, J. P. Lachaux, E. Rodriguez, and J. Martinerie, *Nat. Rev. Neurol.* **2**, 229 (2001).
- [5] G. Buzsáki and A. Draguhn, *Science* **304**, 1926 (2004).
- [6] A. K. Engel, P. Fries, and W. Singer, *Nat. Rev. Neurol.* **2**, 704 (2001).
- [7] A. T. Winfree, *J. Theor. Biol.* **16**, 15 (1967).
- [8] J. Buck, *Q. Rev. Biol.* **63**, 265 (1988).
- [9] Y. Kuramoto, *Lecture Notes in Physics* (Springer, New York, 1975), Vol. 39.
- [10] J. A. Acebrón, L. L. Bonilla, C. J. P. Vicente, F. Ritort, and R. Spigler, *Rev. Mod. Phys.* **77**, 137 (2005).
- [11] F. A. Rodrigues, T. K. DM. Peron, P. Ji, and J. Kurths, *Phys. Rep.* **610**, 1 (2016).
- [12] S. Boccaletti, J. A. Almendral, S. Guan, I. Leyva, Z. Liu, I. Sendiña-Nadal, Z. Wang, and Y. Zou, *Phys. Rep.* **660**, 1 (2016).
- [13] D. S. Lee, *Phys. Rev. E* **72**, 026208 (2005).
- [14] Y. Maistrenko, O. Popovych, O. Burylko, and P. A. Tass, *Phys. Rev. Lett.* **93**, 084102 (2004).
- [15] H. Hong and S. H. Strogatz, *Phys. Rev. Lett.* **106**, 054102 (2011).
- [16] H. Hong and S. H. Strogatz, *Phys. Rev. E* **85**, 056210 (2012).
- [17] H. Daidu, *Theor. Phys.* **77**, 622 (1987).
- [18] D. Iatsenko and P. V. E. McClintock, and A. Stefanovska, *Nat. Commun.* **5**, 4118 (2014).
- [19] S. Watanabe and S. H. Strogatz, *Physica D* **74**, 197 (1994).
- [20] C. Xu, J. Gao, Y. Sun, X. Huang, and Z. Zheng, *Sci. Rep.* **5**, 12039 (2015).
- [21] H. Sakaguchi, *Prog. Theor. Phys.* **79**, 39 (1988).
- [22] E. Montbrió, J. Kurths, and B. Blasius, *Phys. Rev. E* **70**, 056125 (2004).
- [23] Y. Kuramoto and D. Battogtokh, *Nonlinear Phenom. Complex Syst.* **5**, 380 (2002).
- [24] D. M. Abrams and S. H. Strogatz, *Phys. Rev. Lett.* **93**, 174102 (2004).
- [25] D. M. Abrams, R. Mirollo, S. H. Strogatz, and D. A. Wiley, *Phys. Rev. Lett.* **101**, 084103 (2008).
- [26] G. C. Sethia, A. Sen, and F. M. Atay, *Phys. Rev. Lett.* **100**, 144102 (2008).
- [27] I. Omelchenko, O. E. Omel'chenko, P. Hövel, and E. Schöll, *Phys. Rev. Lett.* **110**, 224101 (2013).
- [28] H. Bi, X. Hu, S. Boccaletti, X. Wang, Y. Zou, Z. Liu, and S. Guan, *Phys. Rev. Lett.* **117**, 204101 (2016).
- [29] D. Yuan, M. Zhang, and J. Yang, *Phys. Rev. E* **89**, 012910 (2014).
- [30] T. Qiu, S. Boccaletti, I. Bonamassa, Y. Zou, J. Zhou, Z. Liu, and S. Guan, *Sci. Rep.* **6**, 36713 (2016).
- [31] Y. Xiao, W. Jia, C. Xu, H. Lü, and Z. Zheng, *Europhys. Lett.* **118**, 60005 (2017).
- [32] B. Sonnenschein, T. K. DM. Peron, F. A. Rodrigues, J. Kurths, and L. Schimansky-Geier, *Phys. Rev. E* **91**, 062910 (2015).
- [33] C. Xu, Y. Sun, J. Gao, T. Qiu, Z. Zheng, and S. Guan, *Sci. Rep.* **6**, 21926 (2016).
- [34] C. Xu, J. Gao, H. Xiang, W. Jia, S. Guan, and Z. Zheng, *Phys. Rev. E* **94**, 062204 (2016).
- [35] X. Hu, S. Boccaletti, W. Huang, X. Zhang, Z. Liu, S. Guan, and C.-H. Lai, *Sci. Rep.* **4**, 7262 (2014).
- [36] E. Ott and T. M. Antonsen, *Chaos* **18**, 037113 (2008).
- [37] E. Ott and T. M. Antonsen, *Chaos* **19**, 023117 (2009).
- [38] D. Pazó and E. Montbrió, *Europhys. Lett.* **95**, 60007 (2011).
- [39] L. Basnarkov and V. Urumov, *Phys. Rev. E* **78**, 011113 (2008).
- [40] S. Petkoski, D. Iatsenko, L. Basnarkov, and A. Stefanovska, *Phys. Rev. E* **87**, 032908 (2013).
- [41] D. Iatsenko, S. Petkoski, P. V. E. McClintock, and A. Stefanovska, *Phys. Rev. Lett.* **110**, 064101 (2013).
- [42] J. D. Crawford, *J. Stat. Phys.* **74**, 1047 (1994).
- [43] J. R. Engelbrecht and R. Mirollo, *Phys. Rev. Lett.* **109**, 034103 (2012).
- [44] R. L. Devaney, *An Introduction to Chaotic Dynamical Systems* (Westview Press, Boulder, CO, 2003), pp. 102–112.
- [45] E. Hille, *Ordinary Differential Equations in the Complex Domain* (Dover, New York, 1997), pp. 103–140.
- [46] Y. S. Ilyashenko, D. A. Ryzhov, and D. A. Filimonov, *Funct. Anal. Appl.* **45**, 192 (2011).